Stem Cell Reports
Article

OPEN ACCESS

Mouse Intestinal *Krt15*+ Crypt Cells Are Radio-Resistant and Tumor Initiating

Véronique Giroux,[1,2] Julien Stephan,[1,2] Priya Chatterji,[1,2] Ben Rhoades,[1,2] E. Paul Wileyto,[3] Andres J. Klein-Szanto,[4] Christopher J. Lengner,[5] Kathryn E. Hamilton,[1,2,6] and Anil K. Rustgi[1,2,7,*]

[1]Division of Gastroenterology, Department of Medicine, University of Pennsylvania, Perelman School of Medicine, 951 BRBII/III, 421 Curie Boulevard, Philadelphia, PA 19104, USA
[2]Abramson Cancer Center, University of Pennsylvania, Philadelphia, PA 19104, USA
[3]Department of Biostatistics and Epidemiology, University of Pennsylvania, Philadelphia, PA 19104, USA
[4]Department of Pathology and Cancer Biology Program, Fox Chase Cancer Center, Philadelphia, PA 19111, USA
[5]Department of Biomedical Sciences, School of Veterinary Medicine, Institute for Regenerative Medicine, University of Pennsylvania, Philadelphia, PA 19104, USA
[6]Department of Pediatrics, Division of Gastroenterology, Hepatology and Nutrition, Children's Hospital of Philadelphia, Philadelphia, PA 19104, USA
[7]Department of Genetics, University of Pennsylvania, Philadelphia, PA 19104, USA
*Correspondence: anil2@mail.med.upenn.edu
https://doi.org/10.1016/j.stemcr.2018.04.022

SUMMARY

Two principal stem cell pools orchestrate the rapid cell turnover in the intestinal epithelium. Rapidly cycling *Lgr5*+ stem cells are intercalated between the Paneth cells at the crypt base (CBCs) and injury-resistant reserve stem cells reside above the crypt base. The intermediate filament *Keratin 15* (*Krt15*) marks either stem cells or long-lived progenitor cells that contribute to tissue repair in the hair follicle or the esophageal epithelium. Herein, we demonstrate that *Krt15* labels long-lived and multipotent cells in the small intestinal crypt by lineage tracing. *Krt15*+ crypt cells display self-renewal potential *in vivo* and in 3D organoid cultures. *Krt15*+ crypt cells are resistant to high-dose radiation and contribute to epithelial regeneration following injury. Notably, loss of the tumor suppressor *Apc* in *Krt15*+ cells leads to adenoma and adenocarcinoma formation. These results indicate that *Krt15* marks long-lived, multipotent, and injury-resistant crypt cells that may function as a cell of origin in intestinal cancer.

INTRODUCTION

Epithelial stem cells are multipotent cells with self-renewal capacity that ensure normal epithelial renewal and tissue regeneration in response to injury (e.g., radiation). The intestinal epithelium is highly proliferative, being renewed every few days in the mouse (Bjerknes and Cheng, 1999; Wong et al., 1999; Barker et al., 2012). Two main intestinal stem cell (ISC) pools orchestrate maintenance of the intestinal homeostatic epithelium (Beumer and Clevers, 2016). First, an actively proliferative *Lgr5*+ crypt base columnar cell population (CBC) is driven by the activity of the canonical Wnt pathway (Barker et al., 2007; Kretzschmar and Clevers, 2017). CBCs are also characterized by the expression of *Ascl2*, *Olfm4* (van der Flier et al., 2009), and *Smoc2* (Munoz et al., 2012). Second, a slower cycling reserve crypt stem cell population is located around the +4 position above the crypt base and lacks regulation by the canonical WNT signaling pathway (Sangiorgi and Capecchi, 2008). Specifically, reserve ISCs are marked by CreER insertions into the *Bmi1* (Sangiorgi and Capecchi, 2008) or *Hopx* loci (Takeda et al., 2011), as well as by a *Tert-CreER* transgene mouse (Montgomery et al., 2011). Reserve ISCs were originally associated with label-retention capacities (Potten et al., 1978). The identity and function of intestinal label-retaining cells (LRCs) remain to be fully understood, but recent work shows that intestinal LRCs are secretory precursors of Paneth and enteroendocrine cells, located in the crypt and express *Lgr5* (Buczacki et al., 2013). Subsequent work showed the label-retaining secretory precursor cells to be a distinct population from the reserve ISCs labeled by CreER knockin reporters (Li et al., 2016).

While a body of work has illuminated the distinct nature of these two populations, certain controversies persist. For example, in contrast to *Bmi1-CreER*+ cells, *Bmi1-GFP*+ cells may represent an enteroendocrine progenitor cell population (Jadhav et al., 2017). Furthermore, the heterogeneity of these populations makes interpretation of genetic labeling challenging at times. For example, the RNA binding protein *Mex3a* marks a subpopulation of *Lgr5*+ cells displaying characteristics consistent with reserve-like stem cells (Barriga et al., 2017). Other alleles can broadly mark several cell types; for example, *Lrig1* marks *Lgr5*+ cells (Wong et al., 2012) and reserve ISCs (Powell et al., 2012). However, the populations marked by *Lrig1* can vary greatly depending on whether the readout is endogenous mRNA, protein (which may be antibody dependent), or reporter alleles (Poulin et al., 2014; Powell et al., 2012; Wong et al., 2012). The *Sox9-CreER* allele also marks reserve ISCs and CBCs (Roche et al., 2015). The transcripts of certain reserve stem cell markers are expressed in other crypt cells, notably CBCs, thereby complicating analysis (Li et al., 2014; Munoz et al., 2012; Grun et al., 2015). Nevertheless, single-cell profiling has revealed that *Bmi1-CreER*+ cells and *Hopx-CreER*+ cells

are transcriptionally distinct from *Lgr5-CreER*+ cells and generate CBCs under homeostatic conditions (Li et al., 2014). Also, it has been demonstrated that *Bmi1-CreER*-labeled cells could replenish *Lgr5*+ stem cell population after diphtheria toxin (DT)-mediated ablation (Tian et al., 2011). *Hopx-CreER*-labeled cells could also give rise to CBCs (Takeda et al., 2011).

Interestingly, *Lgr5*+ cells are sensitive to DNA damage and largely ablated with high-dose irradiation (Yan et al., 2012; Hua et al., 2012; Metcalfe et al., 2014; Tao et al., 2015), whereas *Bmi1-CreER* cells (Yan et al., 2012), *Hopx-CreER* cells (Yousefi et al., 2016), and *Lrig1-CreER* cells (Powell et al., 2012) are resistant to high-dose radiation injury. Following radiation, reserve ISCs can give rise to CBCs (Montgomery et al., 2011; Yan et al., 2012; Yousefi et al., 2016). Although *Lgr5*+ cells are sensitive to injury, ablation of *Lgr5*+ cells concomitant with or following radiation results in failed regeneration, suggesting that *de novo* generation of new *Lgr5*+ cells is required for efficient tissue repair (Metcalfe et al., 2014). Interestingly, despite the existence of Wnt-negative, injury-resistant reserve ISCs that contribute to intestinal epithelial regeneration, evidence exists for plasticity in more differentiated intestinal cells. For example, *Dll1*+ secretory progenitor cells can revert to a stem cell state and give rise to *Lgr5*+ cells (van Es et al., 2012). More recently, Asfaha et al. (2015) identified *Krt19+/Lgr5-* radio-resistant and cancer-initiating cells in the small intestine located above the crypt base. Similarly, alkaline-phosphatase-positive transit-amplifying cells can regenerate CBCs after their genetic ablation with *Lgr5-DTR*; however, it remains unknown whether this mechanism is employed in DNA damaging injury under physiological conditions, which might be expected to also ablate the very rapidly cycling transit-amplifying cells (Tetteh et al., 2016).

In the present study, we describe the role of *Keratin 15* (*Krt15*)-labeled cells in the mouse small intestinal epithelium. *Krt15*-labeled cells were characterized initially as stem cells in the hair follicle bulge contributing to wound healing and the development of squamous papilloma (Morris et al., 2004; Ito et al., 2005; Li et al., 2013). We described recently a long-lived *Krt15*+ progenitor cell population in the mouse esophageal epithelium (Giroux et al., 2017). Herein, we identify and describe a long-lived *Krt15*+ cell population in the small intestinal crypt using genetic lineage tracing in mice. *Krt15*+ crypt cells give rise to all the intestinal lineages and have self-renewal capacity. Radio-resistant *Krt15*+ cells contribute to tissue regeneration after radiation-mediated injury. Interestingly, *Apc* loss in *Krt15*+ cells leads to adenoma and adenocarcinoma formation in the small intestine, as well as occasional adenoma formation in the colon, demonstrating the tumor-initiating potential of these cells.

RESULTS

Krt15 Marks Proliferating Cells in the Small Intestinal Crypt

Krt15+ stem/progenitor cells were described originally in the bulge of the hair follicle (Morris et al., 2004) and, more recently, within the basal compartment of the esophageal squamous epithelium (Giroux et al., 2017). Taken together, this suggests an important role for *Krt15*+ cells in the maintenance of squamous epithelia and appendages. In contrast to the multi-layered squamous epithelium in the skin and esophagus, a single layer of the columnar epithelium is present in the mammary gland, pancreas, and intestine. We hypothesized that *Krt15*+ cells in the small intestine might annotate a unique subpopulation of cells with properties that contribute to tissue maintenance and regeneration.

First, we noted that endogenous K15 protein is detected in some crypt cells and occasionally in cells within the villi (Figure 1A) of the small intestine. K15 protein can be detected in all small intestinal segments with slightly higher expression in the ileum. We confirmed these results using a mouse expressing a progesterone receptor (PR)-fused Cre recombinase downstream of *Krt15* promoter (*Krt15-CrePR1* mouse) (Morris et al., 2004) crossed with a reporter mouse expressing the *mTomato-LSL-mGFP* construct from the *Rosa26* locus ($R26^{mT/mG}$) (Muzumdar et al., 2007). A single injection of the PR agonist, RU486, was used for Cre induction and mice were sacrificed 24 hr later to visualize *Krt15*+ (GFP+) cells. *Krt15*+ cells were observed in some crypts and occasionally in the villi of the small intestine (Figure 1B). In the villi, 10% of the GFP+ cells also stained positive for Alcian blue, a goblet cell marker, and 3% also expressed chromogranin A (CHGA), an enteroendocrine cell marker (Figures S1A and S1B), suggesting that the majority of *Krt15*+ cells in the villi are enterocytes. Since the *Krt15*+ villi cells could result from migration of a recombination event in the top of the crypt, we injected *Krt15-CrePR1;*$R26^{mT/mG}$ mice with a single dose of RU486 and mice were sacrificed 8 hr later to minimize the potential for migration of labeled cells. We observed that most labeled cells were located in the lower third of the villi, thereby suggesting that recombination happened in the crypt or at the crypt/villi junction (Figure S1C).

Interestingly, approximately 40% of *Krt15*-labeled cells in the crypt are localized in the stem cell compartment (i.e., +4 position and below) (Figures 1C and S1D). We confirmed that the GFP+ cells located between positions +1 and +4 from the crypt base are not Paneth cells by lysozyme staining (Figures 1D and 1E). GFP can also be detected in some Ki-67+ transit-amplifying cells as a result of possible stem cell division and/or residual *Krt15* promoter activity

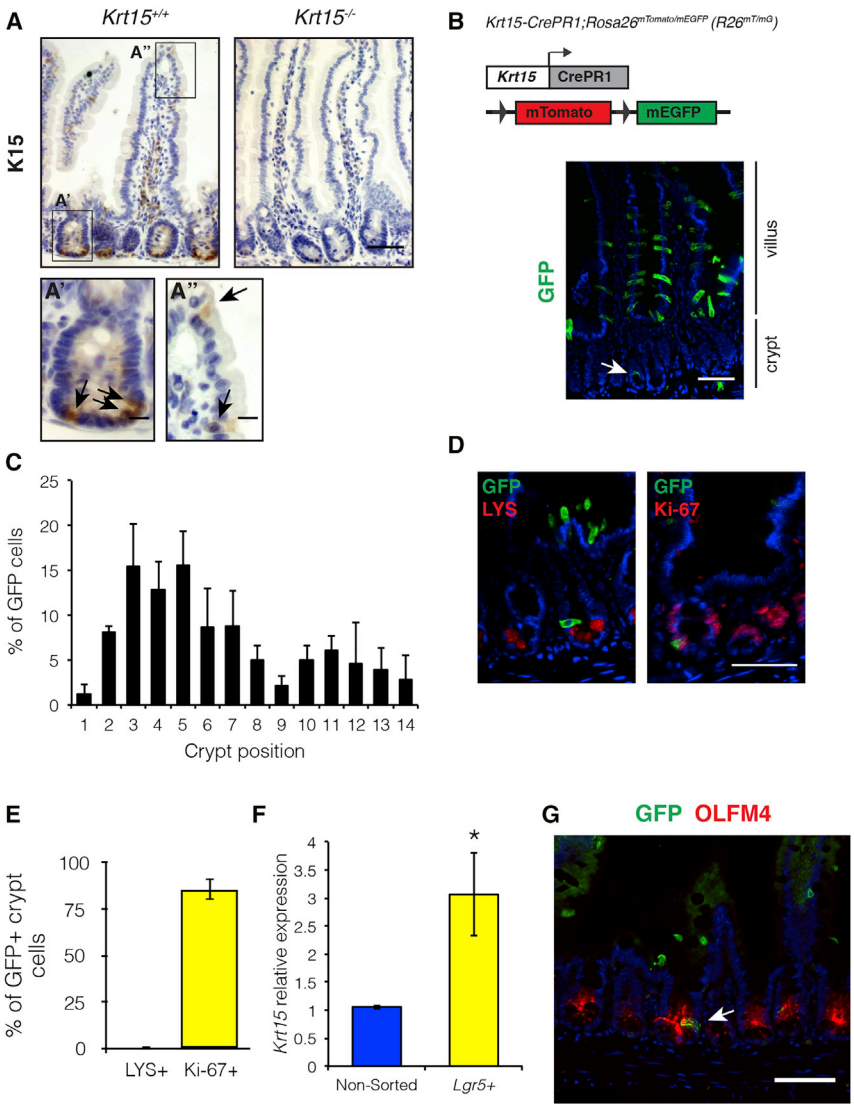

Figure 1. *Krt15* Is Expressed in a Subpopulation of Crypt and Villi Cells

(A) Representative immunohistochemistry (IHC) for K15 in the small intestine (ileum) of adult mice. Small intestinal tissues from *Krt15*$^{-/-}$ mice were used as negative control. Insets for higher magnification of (A′) crypt and (A″) villi staining. Arrows mark cells expressing K15 protein (n = 4 mice).

(B–E) *Krt15-CrePR1;R26*$^{mT/mG}$ mice were administered a single injection of 0.5 mg RU486 to induce Cre recombination and were sacrificed 24 hr later (n = 4 mice). (B) Representative visualization of *Krt15*+ cells by GFP-targeted IF. Arrow marks a GFP + crypt cell. (C) Percentage of GFP+ cells at each crypt position. Graph represents mean ± SEM (n = 3 mice, 50 crypts/mouse were counted). (D and E) Representative co-localization of *Krt15*+ (GFP+) crypt cells with lysozyme (LYS, Paneth cell marker) and Ki-67 (proliferative cell marker). (E) Graph represents percentage of GFP+ crypt cells that are positive for LYS or Ki-67, mean ± SEM (n = 4 mice, 50 crypts/mouse were counted).

(F) *Krt15* mRNA expression in *Lgr5*+ sorted cells versus unsorted cells. Graph represents mean ± SEM (n = 3–5 samples). *Represents statistical significance $p < 0.05$ using the rank-sum (Wilcoxon) test.

(G) Co-localization of *Krt15*+ (GFP+) cells with OLFM4 (CBC marker). Arrow indicates a co-localization event.

Scale bars, 50 μm except for inserts (10 μm). See also Figure S1.

in these cells (Figures 1D and 1E). Interestingly, the +5 to +10 region may contain progenitor/stem cells as illustrated by *Krt19* genetic labeling of multipotent and self-renewing cells (Asfaha et al., 2015). In order to evaluate the crypt cell types that express *Krt15*, we used *Lgr5-EGFP* mice. *Krt15* expression is enriched in *Lgr5*+ cells compared with unsorted crypt cell samples (Figure 1F). Finally, small intestines were harvested from *Krt15-CrePR1;R26*$^{mT/mG}$ mice sacrificed 24 hr after Cre recombination. OLFM4, another marker of *Lgr5*+ stem cells, expression was evaluated. OLFM4 co-expressing GFP+ cells were observed in the bottom of the crypt (Figure 1G). In addition, we investigated the potential overlap between *Krt15*+ cells and +4 reserve ISCs. *Bmi1* and *Hopx* expression is significantly lower in *Krt15*+ cells versus *Krt15*− cells (Figure S1E). These results suggest that *Krt15*-labeled cells in the crypt overlap with CBCs, as well as transit-amplifying cells.

Krt15 Marks Long-Lived Multipotent Crypt Cells with Self-Renewal Capacity

We next performed lineage-tracing experiments using *Krt15-CrePR1;R26*$^{mT/mG}$ mice to investigate the self-renewing capacity of *Krt15*+ crypt cells. Cre recombination was induced by daily injection of RU486 for 5 days (Figure 2A). *Krt15*-derived cells completely labeled the small intestinal crypt-villus axis by 14 days. In the early time points, we rarely observed clusters of cells at the crypt base, but found them mostly in the transit-amplifying zone, which suggests that the *Krt15*+ cells present in that region might be at the origin of the long-term tracing events as was

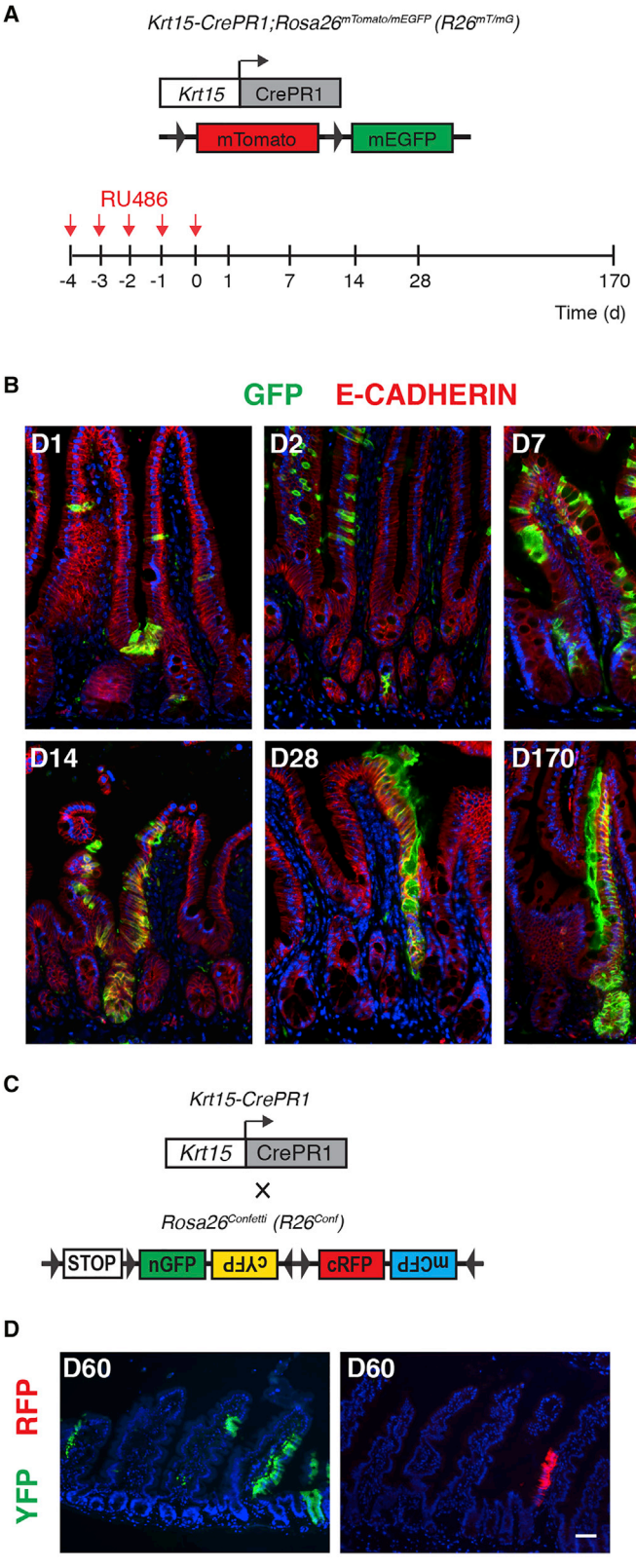

Figure 2. *Krt15* Marks Long-Lived Cells in the Small Intestinal Crypt as Well as Some Cells in the Villi

(A and B) Six- to 8-week-old *Krt15-CrePR1;R26*$^{mT/mG}$ mice were injected daily with 0.5 mg RU486 (PR agonist) to induce Cre recombination for 5 consecutive days and sacrificed at different time points (days post-recombination = D). (B) *Krt15*+ cells were visualized by GFP immunofluorescence (n = 4–7 mice/time point).

(C and D) *Krt15-CrePR1;R26*^{Conf} mice were injected twice a day with 1 mg RU486 for 10 consecutive days to induce recombination. Mice were sacrificed 2 months following recombination (n = 4 mice). (D) Representative images of YFP+ and RFP+ *Krt15*-derived clones visualized by immunofluorescence.

Scale bars, 50 μm. See also Figures S2 and S3.

observed with *Krt19+/Lgr5−* cells (Asfaha et al., 2015). Labeling persists beyond 6 months, thereby suggesting that some *Krt15+* crypt cells are long-lived stem cells (Figures 2B and S2A). Notably, 7% of the crypts were labeled 1 day after the last RU186 injection and 3% after 2 months (Figure S2B). Co-localization of GFP with Ki-67, Alcian blue, chromogranin A, and lysozyme demonstrate that *Krt15+* cells can give rise to proliferative, transit-amplifying cells, goblet cells, enteroendocrine cells, and Paneth cells, respectively (Figures S3A–S3D). *Krt15-CrePR1* mice were also crossed with $Rosa^{Confetti}$ mice. Every *Krt15*-labeled ribbon observed was monochromatic, suggesting that the progeny of *Krt15+* cells may arise from monoclonal units (Figures 2C and 2D). Interestingly, *Krt15* marked clones in the colon epithelium as well (Figure S3E). Taken together, these results indicate that *Krt15* can mark long-lived and multipotent crypt stem cells.

To investigate the self-renewing capacity of *Krt15+* crypt cells, we used *Krt15-CrePR1;*$Rosa26^{LSL\text{-}tdTomato}$ (*Krt15-CrePR1;*$R26^{Tom}$) mice. A single injection of RU486 was used to induce recombination and mice were sacrificed 24 hr later. Crypts were isolated and grown as 3D organoids. *Krt15+* (Tomato+) cells were detected in 3D organoid crypts and these cells expanded to form lineage-traced ribbons as observed *in vivo* (Figure 3A). Interestingly, following 3D organoid passaging, we observed organoids consisting entirely of Tomato+ cells (Figures 3A and 3B). The multipotency of *Krt15+* crypt cells was confirmed in these 3D organoids with Tomato+ proliferative cells, goblet cells, enteroendocrine cells, and Paneth cells (Figure 3C). Furthermore, single crypt cell suspensions were prepared from *Krt15-CrePR1;*$R26^{Tom}$ mice 24 hr following Cre recombination. *Krt15+* cells were able to grow as single cell cultures, suggesting that *Krt15+* crypt cells may display "stemness" features. The organoid formation efficiency of *Krt15+* crypt cells is 0.01%, which is less than the 6% efficiency of *Lgr5+* cells originally reported (Sato et al., 2011), but similar to the 0.01%–1.2% efficiency reported by other groups (Xian et al., 2017; Qi et al., 2017). Of note, these differences in organoid formation capacity of *Krt15+* and *Lgr5+* cells may not correlate with distinct properties *in vivo*. Taken together, these results demonstrate that *Krt15* marks some long-lived and multipotent crypt cells with self-renewing capacity, characteristics consistent with stem cells.

Krt15+ Cells Are Radio-Resistant and Expand in Response to High-Dose Radiation

Reserve stem cells are believed to be radio-resistant and contribute to tissue regeneration following high-dose radiation (Sangiorgi and Capecchi, 2008; Yan et al., 2012; Takeda et al., 2011; Yousefi et al., 2016). Interestingly, *Krt15* mRNA expression is increased in small intestinal cells following irradiation (Figure S4A). Therefore, we investigated the contribution of *Krt15+* cells to tissue regeneration following high-dose γ-irradiation. First, we used *Krt15-CrePR1;*$R26^{mT/mG}$ mice to determine if *Krt15+* cells are resistant to high-dose radiation. Following Cre recombination, mice were subjected to whole-body γ-irradiation (12 Gy) (Figure 4A). After irradiation, *Krt15+* cells were present in the highly proliferative crypts that underwent regeneration and designated as microcolonies (Figure 4B). Five days following irradiation, the percentage of GFP+ cells per crypt was increased in the irradiated mice when compared with non-irradiated mice (Figure 4C). Furthermore, *Krt15+* crypt cells were more proliferative in irradiated animals versus non-irradiated mice (Figures 4D and 4E). These results are consistent with an expansion of *Krt15+* cells in response to irradiation. Finally, we induced Cre recombination in *Krt15-CrePR1;*$R26^{mT/mG}$ mice following whole-body irradiation and noticed that *Krt15+* cells expanded in response to injury in these conditions as well (Figures S4B and S4C). Thus, we demonstrate that *Krt15*-labeled cells are radio-resistant and expand in response to high-dose irradiation.

Due to the multiple roles of keratins in cell migration and proliferation, we sought to characterize the potential role of K15 protein itself in tissue regeneration following injury. We subjected $Krt15^{+/+}$ and $Krt15^{-/-}$ mice to whole-body γ-irradiation (12 Gy) and sacrificed them 5 days later (Figure 5A). Regeneration of the ileum from $Krt15^{-/-}$ mice was impaired following irradiation (Figure 5B). First, fewer residual crypts were observed in the ileum from $Krt15^{-/-}$ compared with $Krt15^{+/+}$ irradiated mice (Figure 5C). Second, crypt length and villus height were both significantly reduced in *Krt15*-deficient mice when compared with $Krt15^{+/+}$ mice (Figures 5D and 5E). Third, crypt regenerative capacity was determined using bromodeoxyuridine (BrdU) incorporation. Crypts containing >10 BrdU+ cells were considered as microcolonies. *Krt15* deficiency significantly reduced the percentage of microcolonies present in the ileum 5 days following irradiation (Figures 5F and 5G). Finally, the percentage of BrdU+ cells per crypt was lower in $Krt15^{-/-}$ versus $Krt15^{+/+}$ ileum. These results suggest a possible role for K15 protein in intestinal tissue regeneration. We appreciate this is likely different from the properties of the *Krt15+* cells.

Apc Loss in *Krt15+* Cells Leads to Adenoma and Adenocarcinoma Formation in the Small Intestine and Colon

Tumor-initiating capacity is an important feature of ISCs. *Lgr5+*, *Lrig1+*, and *Krt19+/Lgr5−* populations have all been described to contain a cell of origin for intestinal tumorigenesis following *Apc* loss (Barker et al., 2009; Powell et al., 2012; Asfaha et al., 2015). Also, *Bmi1-CreER+* cells can form adenomas following induction of a stable form of

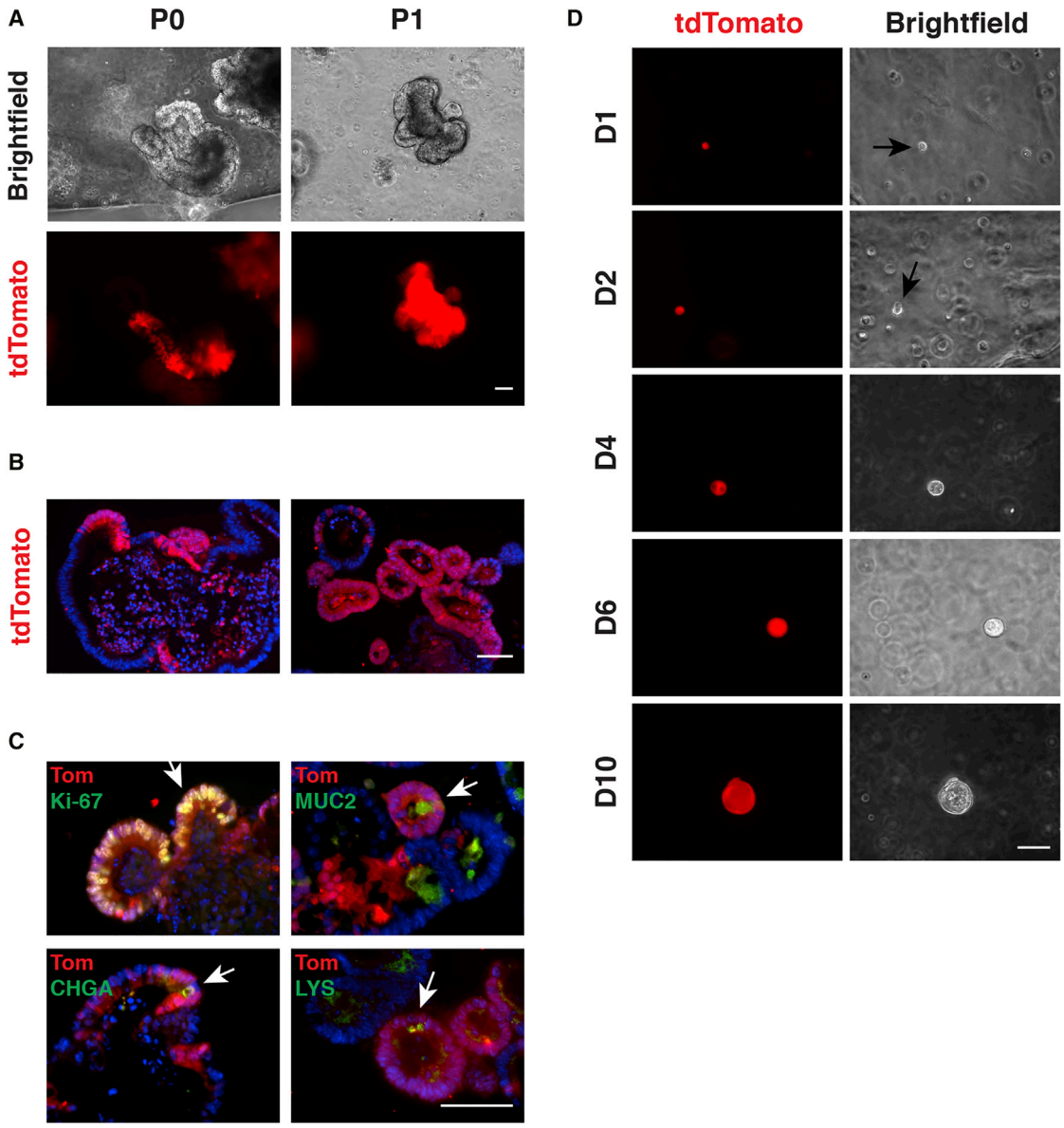

Figure 3. *Krt15* Lineage-Labeled Cells Have Clonogenic Potential

(A–D) *Krt15-CrePR1;R26*^{Tom} mice were injected with 0.5 mg RU486 for Cre induction and sacrificed 24 hr later. 3D organoids were grown from isolated small intestinal (ileum) crypts (P0) and passaged once (P1) (n = 4 mice).

(A and B) Tomato+ (*Krt15*-derived) cells (A) were visualized on live 3D organoids as well as (B) by IF on sections of fixed organoids.

(C) Representative co-staining of Tomato with Ki-67 (proliferative cell marker), Mucin2 (MUC2, goblet cell marker), Chromogranin A (CHGA, enteroendocrine cell marker), and lysozyme (LYS, Paneth cell marker). Arrows mark co-localization.

(D) Single suspensions of Tomato+ cells were sorted and seeded in Matrigel and grown for 10 days. Representative pictures of 3D organoids growing from *Krt15*+ cells at different time points following seeding (D = days) (n = 4 mice, 4 experimental replicates/mouse). Arrows mark spheres that are forming.

Scale bars, 50 μm.

β-catenin in these cells (Sangiorgi and Capecchi, 2008). In order to determine if *Krt15*+ cells can initiate tumor formation in the intestine, we bred *Apc*$^{fl/fl}$ mice with the *Krt15-CrePR1;R26*$^{mT/mG}$ mice. Cre recombination was induced using daily injection of 0.5 mg RU486 for 5 consecutive days. Mice were sacrificed 6 months after Cre recombination or at prior time points if severe weight loss necessitated sacrifice (Figure 6A). Gross lesions were observed in the

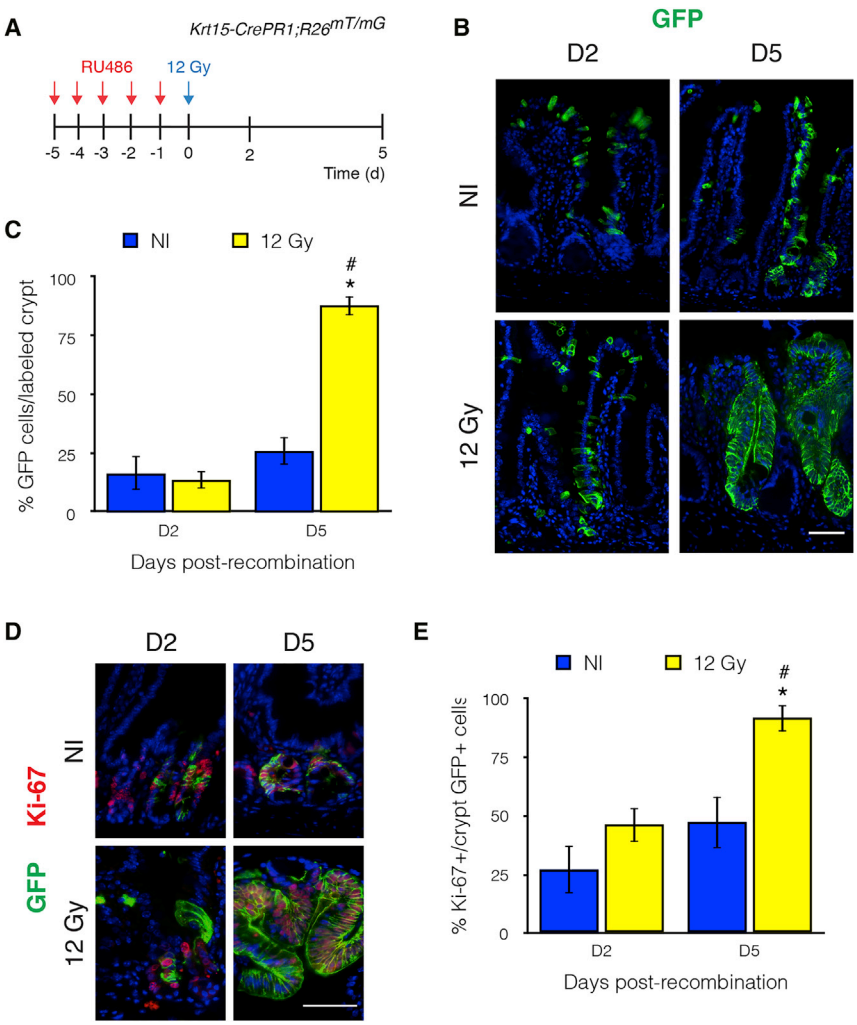

Figure 4. *Krt15*+ Cells Are Radio-Resistant and Contribute to Tissue Regeneration

(A–E) *Krt15-CrePR1;R26*$^{mT/mG}$ mice were treated with 0.5 mg RU486 daily for 5 consecutive days to induce Cre recombination. Mice were subjected or not to 12 Gy whole-body γ-irradiation 1 day after Cre induction and sacrificed 2 (D2) or 5 days (D5) after irradiation (NI = Non-irradiated) (n = 3–4 mice/group). (B) GFP labeling of *Krt15*-derived cells during regeneration following irradiation. (C) Percentage of GFP+ cells in labeled crypts following irradiation in comparison to normal conditions. Graph represents mean ± SEM (n = 3–4 mice/group). *Represents statistical significance with $p < 0.05$ versus D2 and $^{\#}p < 0.05$ versus non-irradiated animals, using Student's t test). (D and E) Ki-67 staining of GFP+ regenerative crypts. (E) Percentage of Ki-67 positivity in crypt GFP+ cells. Graph represents mean ± SEM (n = 3–4 mice/group, 50 crypts/mouse were analyzed). *Represents statistical significance with $p < 0.05$ versus D2 and $^{\#}p < 0.05$ versus non-irradiated animals, using Student's t test.

Scale bars, 50 μm. See also Figure S4.

intestinal tract of *Krt15-CrePR1;Apc*$^{fl/fl}$*;R26*$^{mT/mG}$ mice but not in control mice (n = 8 mice) (Figure 6B). All mice developed lesions in the small intestine while colon lesions were observed in 37% of the mice (Figure 6C). Mice developed between 4 and 33 tumors measuring on average 3.17 mm. Most observed lesions were adenomas, but invasive adenocarcinomas were occasionally observed. Interestingly, half of the *Krt15-CrePR1;Apc*$^{fl/fl}$*;R26*$^{mT/mG}$ mice developed at least one adenocarcinoma (Figures 6D and 6E). The lesions were highly proliferative, as demonstrated by a large number of Ki-67+ cells (Figure 6F) and had also evidence of nuclear β-catenin staining (Figure 6G). *TP53* mutations are observed at later stages of colon cancer and typically lead to nuclear accumulation of p53 (Fearon and Vogelstein, 1990). We observed nuclear p53 staining in some tumor regions (Figure 6H). These results demonstrate that tumor-initiating cells exist within the *Krt15*+ population, and lesions derived from *Krt15*+ cells can even progress to invasive adenocarcinoma.

DISCUSSION

We report that some *Krt15*+ lineage-labeled small intestinal crypt cells have self-renewal capacity, give rise to all differentiated cell lineages, and participate in tissue regeneration following high-dose radiation injury. In combination with *Apc* loss, *Krt15*+ cells can give rise to adenomas and even adenocarcinomas. While the spatial localization of *Krt15*+ cells in intestinal crypts is not limited to CBCs or +4 ISCs, our results suggest that *Krt15* could annotate a subpopulation of *Lgr5*+ cells.

Krt15+ cells are predominantly detected at the crypt base where *Lgr5*+ stem cells reside (Barker et al., 2007), while the *Bmi1*+ or *Hopx*+ reserve stem cells are localized at the +4 position above the crypt base (Sangiorgi and Capecchi, 2008; Takeda et al., 2011). Sorted *Lgr5*+ cells also harbor higher *Krt15* mRNA expression and some *Krt15*-labeled cells also express OLFM4. These results suggest at least partial overlap between *Krt15*+ cells and *Lgr5*+ cells. Analysis of

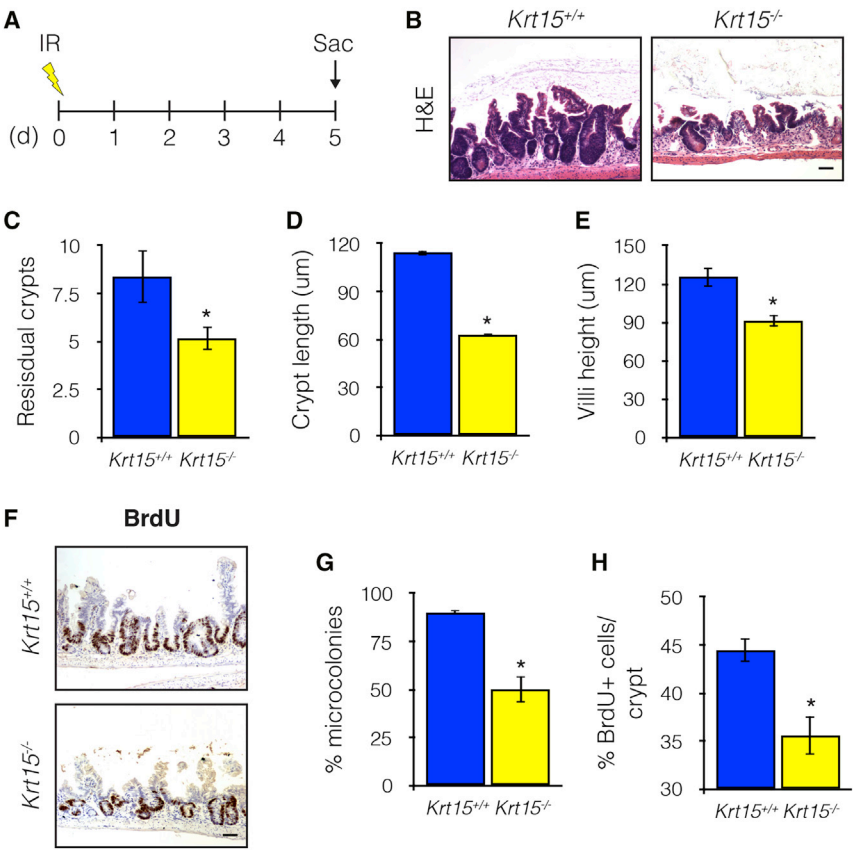

Figure 5. *Krt15* Loss Impairs Intestinal Tissue Regeneration Following Gamma-Irradiation

(A–H) Six- to 8-week-old *Krt15*$^{+/+}$ and *Krt15*$^{-/-}$ mice were subjected to 12 Gy whole-body γ-irradiation and sacrificed 5 days later. Tissue injury and regeneration were compared in ileal sections.

(B) Representative H&E staining from ileal sections.

(C) Residual crypts by high-power field (HPF) images were quantified, graph represents mean ± SEM (n = 3–4 mice/group, 25 HPFs/mouse were analyzed. *Represents statistical significance with $p < 0.05$ using Student's t test).

(D and E) Crypt length (D) and villi height (E) were measured in ileal sections, graph represents mean ± SEM (n = 3–4 mice/group, 50 crypts and villus/mouse were measured. *Represents statistical significance with $p < 0.05$ using Student's t test).

(F–H) Mice were injected with BrdU 1.5 hr prior to sacrifice and BrdU+ cells were detected by IHC.

(G) The percentage of microcolonies (crypt with >10 BrdU + cells/total number of crypts by HPF) was quantified, graph represents mean ± SEM (n = 3–4 mice/group, 25 HPFs/mouse were analyzed. *Represents statistical significance with $p < 0.05$ using Student's t test).

(H) The percentage of BrdU+ cells/crypt was quantified, graph represents mean ± SEM (n = 3–4 mice/group, 50 crypts/mouse were analyzed. *Represents statistical significance with $p < 0.05$ using Student's t test).

Scale bars, 50 μm.

published datasets also suggests upregulation of *Krt15* transcript in *Lgr5*+ cells versus *Lgr5*− cells (1.00842 versus 0.0258, p = 0.052) (Yan et al., 2012). Some *Krt15*+ cells are located above the +4 position, in the transit-amplifying zone similar to *Krt19*+/*Lgr5*− stem-like cells (Asfaha et al., 2015). This suggests heterogeneity throughout the *Krt15*+ crypt population. Nevertheless, we observed multipotency and self-renewing capacity in *Krt15*+ cells, indicating that at least some *Krt15*+ crypt cells have properties consistent with stem cells or long-lived progenitor cells.

Lgr5+ CBCs are thought to be highly sensitive to high-dose radiation, while the reserve stem cells are resistant to such an insult (Hua et al., 2012; Metcalfe et al., 2014; Yan et al., 2012; Tao et al., 2015). Herein, we demonstrate that intestinal *Krt15*+ crypt cells are resistant to high-dose radiation. Due to the possible overlap between *Krt15*+ cells and *Lgr5*+ cells, *Krt15* could mark a subpopulation of *Lgr5*+ cells that could be resistant to radiation. Although radiation ablates the vast majority of *Lgr5*+ cells, a small fraction of *Lgr5*+ cells persists (Yan et al., 2012; Tao et al., 2015; Hua et al., 2012; Metcalfe et al., 2014) and these might be marked by *Krt15* promoter activity. Recently, a subpopulation of *Lgr5*+ cells was described as expressing a high level of *Mex3a*, suggesting heterogeneity in the *Lgr5*+ cell population (Barriga et al., 2017). However, *Mex3a* is not differentially expressed between *Krt15*+ and *Krt15*− cells (data not shown). Furthermore, analysis of published datasets revealed no enrichment of *Krt15* in previously described *Lgr5*+ subpopulations of cells (Barriga et al., 2017; Yan et al., 2012; Munoz et al., 2012). *Krt15*+ cells located above the +4 position might also be radio-resistant, as has been described for the similarly located *Krt19*+/*Lgr5*− cells(Asfaha et al., 2015).

Inadequate regeneration following radiation was observed in the *Krt15*-deficient mice, suggesting a possible role for the K15 protein. Keratins confer structural support in epithelial cells and are also involved in sensing cues from the microenvironment. Keratins form a strong complex with integrins and other extracellular-matrix-associated proteins. It is believed that the stem cell niche often

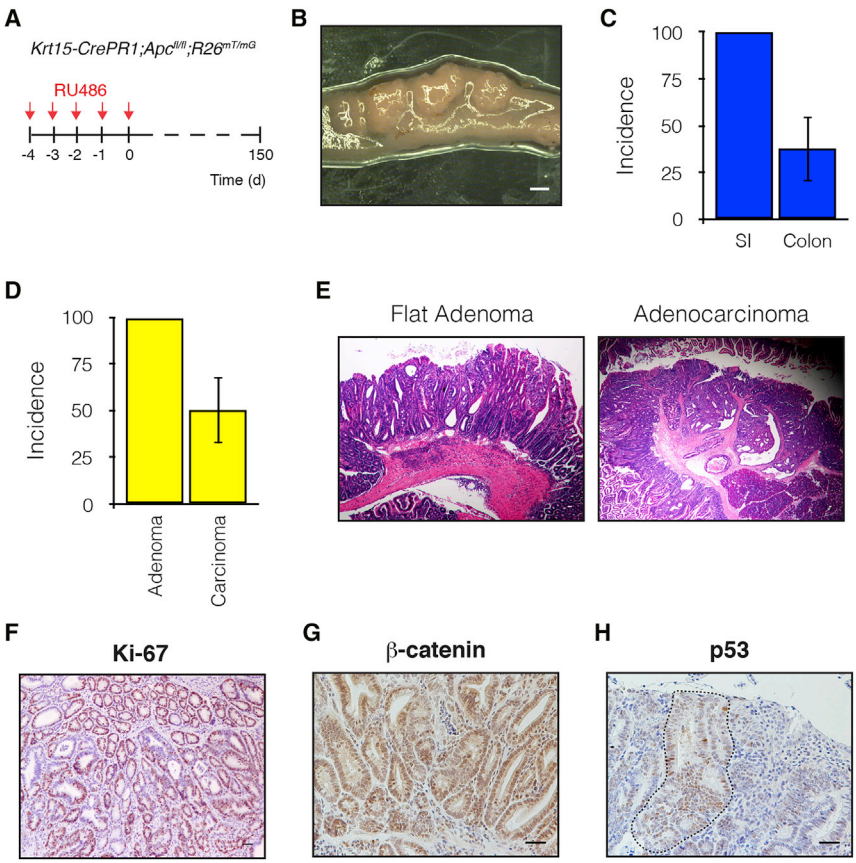

Figure 6. *Krt15*+ Cells Are Tumor-Initiating Cells in the Intestine

(A) *Krt15-CrePR1;Apc*$^{fl/fl}$*;R26*$^{mT/mG}$ mice were injected daily with 0.5 mg RU486 for 5 consecutive days to induce Cre recombination and mice were sacrificed when sick or 150 days following Cre induction (n = 8 mice).

(B) Representative image of small intestinal tumors observed in *Krt15-CrePR1;Apc*$^{fl/fl}$*;R26*$^{mT/mG}$ mice. Scale bar, 1 mm.

(C) Incidence of lesions in small intestine (SI) and colon of *Krt15-CrePR1;Apc*$^{fl/fl}$*;R26*$^{mT/mG}$ mice (n = 8 mice).

(D) Incidence of adenomas and adenocarcinomas in *Krt15-CrePR1;Apc*$^{fl/fl}$*;R26*$^{mT/mG}$ mice (n = 8 mice).

(E–H) Representative histology of flat adenoma and invasive adenocarcinoma observed in *Krt15-CrePR1;Apc*$^{fl/fl}$*;R26*$^{mT/mG}$ mice. (F) Ki-67, (G) β-catenin, and (H) p53 staining of small intestinal tumors observed in *Krt15-CrePR1;Apc*$^{fl/fl}$*;R26*$^{mT/mG}$ mice. Scale bar, 50 μm.

involves extrinsic cells or extracellular proteins or molecules that will modify the immediate environment of stem cells. Interestingly, integrin signaling has been shown to be essential for ISC maintenance and proliferation in *Drosophila* (Lin et al., 2013; You et al., 2014). It has been shown that keratins can interact with several kinases and other cytoplasmic proteins to regulate cell proliferation and cell metabolism (Bragulla and Homberger, 2009). For example, K19 interacts with β-catenin/RAC1 complex in breast cancer cells inducing nuclear translocation of β-catenin(Saha et al., 2017). K8 and K18 interact with TNFR2 affecting nuclear factor κB signaling (Caulin et al., 2000) and K17 regulates the AKT/mTOR pathway by interacting with 14-3-3σ, resulting in protein synthesis and cell growth upregulation (Kim et al., 2006). Herein, we demonstrate that mice lacking *Krt15* recover more slowly in response to high-dose radiation, thereby suggesting that K15 protein could also play a role in tissue regeneration.

Several studies have been conducted to identify the cell of origin of intestinal cancers. *Apc* loss in *Lgr5-CreER*+ cells (Barker et al., 2009; Asfaha et al., 2015), *Lrig1-CreER*+ cells (Powell et al., 2012, 2014), and *Krt19-CreER*+ cells (Asfaha et al., 2015) lead to adenoma formation. Adenomas are also observed following induction of stable β-catenin in *Bmi1-CreER*+ cells (Sangiorgi and Capecchi, 2008). None of these studies have reported progression to adenocarcinoma. Herein, we observed that mice harboring *Apc* loss in *Krt15-CrePR1*+ cells develop adenomas and invasive adenocarcinomas. These results suggest that *Krt15*+ cells are tumor-initiating cells, spanning benign to malignant lesions. Loss of *Apc* in *Krt15*+ cells leads to more severe lesions that what was reported for *Lgr5*+, *Lrig1*+, or *Krt19*+ cells. Mice presenting *Apc* loss in *Krt15*+ cells survive longer in contrast to other reported mice, which could mean that the latter mice do not survive long enough to display adenocarcinomas. Alternatively, this could suggest different cells of origin for adenomas and adenocarcinomas. Interestingly, in inherited colon cancer syndromes, one may see variable presentation of adenomatous polyps or hamartomatous polyps with or without progression to colon cancer (Rustgi, 2007) and this may underlie the potential heterogeneity of cells of origin that may be implied in the various mouse models. Finally, extensive adenoma formation like observed in mice carrying loss of *Apc* in *Lgr5*+ cells could require culling before cancer progression.

The lesions formed by *Krt15*+ cells most likely originate from the cells located at the crypt base and/or those located in the transit-amplifying zone. We also cannot exclude the possibility that *Krt15*+ villi cells might have given rise to the lesions since it has been demonstrated that cells in the villi can initiate tumorigenesis (Davis et al., 2015). In that model, aberrant expression of the BMP antagonist, GREM1, led to formation of intestinal tumors histologically similar to polyps observed in hereditary mixed polyposis syndrome. Nevertheless, *Krt15-CrePR1;Apc*$^{fl/fl}$ mice might represent a new mouse model for intestinal cancer as a foundation for understanding the interrelationship between normal intestinal cells and malignant transformation.

Overall, we demonstrate that *Krt15*+ crypt cells are self-renewing, multipotent, radio-resistant, and tumor initiating in concert with *Apc* loss. *Krt15*+ cells could represent a radio-resistant subpopulation of *Lgr5*+ cells. RNA profiling of *Krt15*+ esophageal long-lived progenitor cells revealed enrichment for gene sets associated with Wnt/β-catenin pathway and DNA repair (Giroux et al., 2017). It is possible, if not likely, that the Wnt/β-catenin pathway is involved in the proliferative capacity of *Krt15*+ intestinal crypt cells and their tumor-initiating capacities. Furthermore, *Krt15*+ cells could also display higher DNA repair capacity to ensure genomic stability in response to radiation by example.

EXPERIMENTAL PROCEDURES

Mouse Experimental Design

Krt15-CrePR1 (Morris et al., 2004) and *Krt15*$^{-/-}$ mice were provided by Dr. George Cotsarelis (University of Pennsylvania). *Rosa26*$^{mTomato/mGFP}$ (*R26*$^{mT/mG}$) mice (Muzumdar et al., 2007) were purchased from Jackson Laboratories. *Rosa26*^{Confetti} (*R26*^{Conf}) mice were provided by Dr. Ben Stanger (University of Pennsylvania). *Rosa26*$^{LSL\text{-}tdTomato}$ (*R26*^{Tom}) mice were provided by Dr. Christopher Lengner (University of Pennsylvania). *Apc*$^{fl/fl}$ mice were obtained from the NCI Mouse Repository (Kuraguchi et al., 2006). All experiments were performed with 6- to 10-week-old mice. Intraperitoneal injection of PR agonist, RU486, was performed to induce Cre recombination. The Institutional Animal Care and Use Committee of the University of Pennsylvania approved all animal studies. Detailed information regarding mouse experimental design and treatment are in the Supplemental Information.

Irradiation

Six- to eight-week-old mice were subjected to 12 Gy whole-body gamma-irradiation (Gammacell 40 Cesium 137 Irradiation Unit). Mice were sacrificed 5 days later, and the small intestines were harvested and fixed for histology. Surviving crypts, crypt length, and villi height were measured on H&E-stained ileum sections. Twenty-five high-magnification fields were analyzed for each mouse and a minimum of 100 crypts or villi were measured for each mouse.

Single-Cell Isolation

Crypt single cells were isolated as described previously (Hamilton et al., 2015). Briefly, the small intestine was opened longitudinally and washed with cold PBS. Tissue was incubated 20 min on ice in PBS-EDTA-DTT. Tissues were then incubated in PBS-EDTA at 37°C. Crypts were isolated from the epithelial fraction using a 70-μm filter. Crypts were then dissociated to a single-cell suspension using PBS/dispase at 37°C.

Crypt Isolation and 3D Organoid Culture

Crypts were isolated from the mouse small intestinal ileum. Tissues were chilled in Ca^{2+}-Mg^{2+}-free Hank's balanced salt solution (CMF-HBSS) with 1 mM N-acetyl-cysteine (NAC). Tissues were then incubated in CMF-HBSS/1 mM NAC/10 mM EDTA for 45 min at 4°C. Epithelial cells were then dissociated through vortexing/resting cycles. Crypts were separated from epithelial dissociation with a 70-μm filter. Crypts were pelleted and resuspended in Basal Media (Advanced DMEM/F12, 2 mM Glutamax, 10 mM HEPES, 1× penicillin/streptomycin, 5 μM CHIR99021 [Cayman Chemical], 1 mM NAC, 1× N2 Supplement [Gibco], and 1× B27 Supplement [Gibco]). Approximately 500 crypts were then embedded in 80% Matrigel/20% ENR (Basal Media; 50 ng/mL recombinant mouse epidermal growth factor [R&D Systems] and 1% Noggin/R-Spondin conditioned media). Enteroids were cultured in ENR.

Fluorescence-Activated Cell Sorting

Crypt single-cell suspension was prepared from *Krt15-CrePR1;R26*^{Tom} small intestines as described above. The fluorescence-activated cell sorting sorter Jazz (BD Biosciences) was used to sort Tomato+ and Tomato-crypt cells. Sorting was conducted at the University of Pennsylvania Flow Cytometry and Cell Sorting Facility. Cells were sorted in Advanced DMEM/F12 media supplemented with 1× penicillin-streptomycin, 1× GlutaMAX, 1× HEPES, and 10 μM Rock inhibitor Y27632. Cells were then used for 3D organoid formation or RNA extraction.

Details on mouse experimental design, immunohistochemistry and immunofluorescence, RNA extraction, qPCR, and statistical analyses are available in Supplemental Information.

SUPPLEMENTAL INFORMATION

Supplemental Information includes Supplemental Experimental Procedures, four figures, and two tables and can be found with this article online at https://doi.org/10.1016/j.stemcr.2018.04.022.

AUTHOR CONTRIBUTIONS

V.G., K.E.H., C.J.L., and A.K.R. designed the study. V.G., J.S., and P.C. performed the experiments. B.R. maintained the mouse colony. E.P.W. assisted with statistical analysis. A.J.K.-S. assisted with histology analysis. V.G. and A.K.R. wrote the manuscript. J.S. is currently affiliated with University Medicine Greifswald (Department of Medicine).

ACKNOWLEDGMENTS

We are grateful to members of the Rustgi lab for discussions and comments on the manuscript. We thank the Molecular Pathology

and Imaging Core, Human Microbial and Analytic Depository Core, Cell Culture and iPS Core, Genetic and Modified Mouse Core, and FACS/sorting Core facilities (University of Pennsylvania). We thank Dr. George Cotsarelis (University of Pennsylvania) for *Krt15-CrePR1* and *Krt15*$^{-/-}$ mice, Dr. Ben Stanger (University of Pennsylvania) for *Rosa*^{Confetti} mice, and Dr. Christopher Lengner (University of Pennsylvania) for *Rosa*$^{LSL\text{-}tdTomato}$ mice. We thank MaryAnn Crissey and Dr. John Lynch for providing *Lgr5+* sorted cells. This work was supported by NCI P01-CA098101 (V.G., A.J.K.-S., and A.K.R.), NIH/National Institute of Diabetes and Digestive and Kidney Diseases (NIDDK) P30-DK050306 Center of Molecular Studies in Digestive and Liver Diseases, NIH R01-DK056645 (A.K.R.), American Cancer Society (A.K.R.), Fonds de recherche en santé du Québec P-Giroux-27692 and P-Giroux-31601 (V.G.), NIH NIDDK K01-DK100485 (K.E.H.), and Crohn's and Colitis Foundation Career Development Award (K.E.H.).

Received: July 7, 2017
Revised: April 23, 2018
Accepted: April 24, 2018
Published: May 24, 2018

REFERENCES

Asfaha, S., Hayakawa, Y., Muley, A., Stokes, S., Graham, T.A., Ericksen, R.E., Westphalen, C.B., von Burstin, J., Mastracci, T.L., Worthley, D.L.,, et al. (2015). Krt19(+)/Lgr5(-) cells are radioresistant cancer-initiating stem cells in the colon and intestine. Cell Stem Cell *16*, 627–638.

Barker, N., Ridgway, R.A., van Es, J.H., van de Wetering, M., Begthel, H., van den Born, M., Danenberg, E., Clarke, A.R., Sansom, O.J., and Clevers, H. (2009). Crypt stem cells as the cells-of-origin of intestinal cancer. Nature *457*, 608–611.

Barker, N., van Es, J.H., Kuipers, J., Kujala, P., van den Born, M., Cozijnsen, M., Haegebarth, A., Korving, J., Begthel, H., Peters, P.J., et al. (2007). Identification of stem cells in small intestine and colon by marker gene Lgr5. Nature *449*, 1003–1007.

Barker, N., van Oudenaarden, A., and Clevers, H. (2012). Identifying the stem cell of the intestinal crypt: strategies and pitfalls. Cell Stem Cell *11*, 452–460.

Barriga, F.M., Montagni, E., Mana, M., Mendez-Lago, M., Hernando-Momblona, X., Sevillano, M., Guillaumet-Adkins, A., Rodriguez-Esteban, G., Buczacki, S.J.A., Gut, M., et al. (2017). Mex3a marks a slowly dividing subpopulation of Lgr5+ intestinal stem cells. Cell Stem Cell *20*, 801–816.e7.

Beumer, J., and Clevers, H. (2016). Regulation and plasticity of intestinal stem cells during homeostasis and regeneration. Development *143*, 3639–3649.

Bjerknes, M., and Cheng, H. (1999). Clonal analysis of mouse intestinal epithelial progenitors. Gastroenterology *116*, 7–14.

Bragulla, H.H., and Homberger, D.G. (2009). Structure and functions of keratin proteins in simple, stratified, keratinized and cornified epithelia. J. Anat. *214*, 516–559.

Buczacki, S.J., Zecchini, H.I., Nicholson, A.M., Russell, R., Vermeulen, L., Kemp, R., and Winton, D.J. (2013). Intestinal label-retaining cells are secretory precursors expressing Lgr5. Nature *495*, 65–69.

Caulin, C., Ware, C.F., Magin, T.M., and Oshima, R.G. (2000). Keratin-dependent, epithelial resistance to tumor necrosis factor-induced apoptosis. J. Cell Biol. *149*, 17–22.

Davis, H., Irshad, S., Bansal, M., Rafferty, H., Boitsova, T., Bardella, C., Jaeger, E., Lewis, A., Freeman-Mills, L., Giner, F.C., et al. (2015). Aberrant epithelial GREM1 expression initiates colonic tumorigenesis from cells outside the stem cell niche. Nat. Med. *21*, 62–70.

Fearon, E.R., and Vogelstein, B. (1990). A genetic model for colorectal tumorigenesis. Cell *61*, 759–767.

Giroux, V., Lento, A.A., Islam, M., Pitarresi, J.R., Kharbanda, A., Hamilton, K.E., Whelan, K.A., Long, A., Rhoades, B., Tang, Q., et al. (2017). Long-lived keratin 15+ esophageal progenitor cells contribute to homeostasis and regeneration. J. Clin. Invest. *127*, 2378–2391.

Grun, D., Lyubimova, A., Kester, L., Wiebrands, K., Basak, O., Sasaki, N., Clevers, H., and van Oudenaarden, A. (2015). Single-cell messenger RNA sequencing reveals rare intestinal cell types. Nature *525*, 251–255.

Hamilton, K.E., Crissey, M.A., Lynch, J.P., and Rustgi, A.K. (2015). Culturing adult stem cells from mouse small intestinal crypts. Cold Spring Harb. Protoc. *2015*, 354–358.

Hua, G., Thin, T.H., Feldman, R., Haimovitz-Friedman, A., Clevers, H., Fuks, Z., and Kolesnick, R. (2012). Crypt base columnar stem cells in small intestines of mice are radioresistant. Gastroenterology *143*, 1266–1276.

Ito, M., Liu, Y., Yang, Z., Nguyen, J., Liang, F., Morris, R.J., and Cotsarelis, G. (2005). Stem cells in the hair follicle bulge contribute to wound repair but not to homeostasis of the epidermis. Nat. Med. *11*, 1351–1354.

Jadhav, U., Saxena, M., O'Neill, N.K., Saadatpour, A., Yuan, G.C., Herbert, Z., Murata, K., and Shivdasani, R.A. (2017). Dynamic reorganization of chromatin accessibility signatures during dedifferentiation of secretory precursors into Lgr5+ intestinal stem cells. Cell Stem Cell *21*, 65–77.e5.

Kim, S., Wong, P., and Coulombe, P.A. (2006). A keratin cytoskeletal protein regulates protein synthesis and epithelial cell growth. Nature *441*, 362–365.

Kretzschmar, K., and Clevers, H. (2017). Wnt/beta-catenin signaling in adult mammalian epithelial stem cells. Dev. Biol. *428*, 273–282.

Kuraguchi, M., Wang, X.P., Bronson, R.T., Rothenberg, R., Ohene-Baah, N.Y., Lund, J.J., Kucherlapati, M., Maas, R.L., and Kucherlapati, R. (2006). Adenomatous polyposis coli (APC) is required for normal development of skin and thymus. PLoS Genet. *2*, e146.

Li, N., Nakauka-Ddamba, A., Tobias, J., Jensen, S.T., and Lengner, C.J. (2016). Mouse label-retaining cells are molecularly and functionally distinct from reserve intestinal stem cells. Gastroenterology *151*, 298–310.e7.

Li, N., Yousefi, M., Nakauka-Ddamba, A., Jain, R., Tobias, J., Epstein, J.A., Jensen, S.T., and Lengner, C.J. (2014). Single-cell analysis of proxy reporter allele-marked epithelial cells establishes intestinal stem cell hierarchy. Stem Cell Reports *3*, 876–891.

Li, S., Park, H., Trempus, C.S., Gordon, D., Liu, Y., Cotsarelis, G., and Morris, R.J. (2013). A keratin 15 containing stem cell population from the hair follicle contributes to squamous papilloma development in the mouse. Mol. Carcinog. *52*, 751–759.

Lin, G., Zhang, X., Ren, J., Pang, Z., Wang, C., Xu, N., and Xi, R. (2013). Integrin signaling is required for maintenance and proliferation of intestinal stem cells in *Drosophila*. Dev. Biol. *377*, 177–187.

Metcalfe, C., Kljavin, N.M., Ybarra, R., and de Sauvage, F.J. (2014). Lgr5+ stem cells are indispensable for radiation-induced intestinal regeneration. Cell Stem Cell *14*, 149–159.

Montgomery, R.K., Carlone, D.L., Richmond, C.A., Farilla, L., Kranendonk, M.E., Henderson, D.E., Baffour-Awuah, N.Y., Ambruzs, D.M., Fogli, L.K., Algra, S., et al. (2011). Mouse telomerase reverse transcriptase (mTert) expression marks slowly cycling intestinal stem cells. Proc. Natl. Acad. Sci. USA *108*, 179–184.

Morris, R.J., Liu, Y., Marles, L., Yang, Z., Trempus, C., Li, S., Lin, J.S., Sawicki, J.A., and Cotsarelis, G. (2004). Capturing and profiling adult hair follicle stem cells. Nat. Biotechnol. *22*, 411–417.

Munoz, J., Stange, D.E., Schepers, A.G., van de Wetering, M., Koo, B.K., Itzkovitz, S., Volckmann, R., Kung, K.S., Koster, J., Radulescu, S., et al. (2012). The Lgr5 intestinal stem cell signature: robust expression of proposed quiescent '+4' cell markers. EMBO J. *31*, 3079–3091.

Muzumdar, M.D., Tasic, B., Miyamichi, K., Li, L., and Luo, L. (2007). A global double-fluorescent cre reporter mouse. Genesis *45*, 593–605.

Potten, C.S., Hume, W.J., Reid, P., and Cairns, J. (1978). The segregation of DNA in epithelial stem cells. Cell *15*, 899–906.

Poulin, E.J., Powell, A.E., Wang, Y., Li, Y., Franklin, J.L., and Coffey, R.J. (2014). Using a new Lrig1 reporter mouse to assess differences between two Lrig1 antibodies in the intestine. Stem Cell Res. *13*, 422–430.

Powell, A.E., Vlacich, G., Zhao, Z.Y., McKinley, E.T., Washington, M.K., Manning, H.C., and Coffey, R.J. (2014). Inducible loss of one Apc allele in Lrig1-expressing progenitor cells results in multiple distal colonic tumors with features of familial adenomatous polyposis. Am. J. Physiol. Gastrointest. Liver Physiol. *307*, G16–G23.

Powell, A.E., Wang, Y., Li, Y., Poulin, E.J., Means, A.L., Washington, M.K., Higginbotham, J.N., Juchheim, A., Prasad, N., Levy, S.E., et al. (2012). The pan-ErbB negative regulator Lrig1 is an intestinal stem cell marker that functions as a tumor suppressor. Cell *149*, 146–158.

Qi, Z., Li, Y., Zhao, B., Xu, C., Liu, Y., Li, H., Zhang, B., Wang, X., Yang, X., Xie, W., et al. (2017). BMP restricts stemness of intestinal Lgr5(+) stem cells by directly suppressing their signature genes. Nat. Commun. *8*, 13824.

Roche, K.C., Gracz, A.D., Liu, X.F., Newton, V., Akiyama, H., and Magness, S.T. (2015). SOX9 maintains reserve stem cells and preserves radioresistance in mouse small intestine. Gastroenterology *149*, 1553–1563.e10.

Rustgi, A.K. (2007). The genetics of hereditary colon cancer. Genes Dev. *21*, 2525–2538.

Saha, S.K., Choi, H.Y., Kim, B.W., Dayem, A.A., Yang, G.M., Kim, K.S., Yin, Y.F., and Cho, S.G. (2017). KRT19 directly interacts with beta-catenin/RAC1 complex to regulate NUMB-dependent NOTCH signaling pathway and breast cancer properties. Oncogene *36*, 332–349.

Sangiorgi, E., and Capecchi, M.R. (2008). Bmi1 is expressed in vivo in intestinal stem cells. Nat. Genet. *40*, 915–920.

Sato, T., van Es, J.H., Snippert, H.J., Stange, D.E., Vries, R.G., van den Born, M., Barker, N., Shroyer, N.F., van de Wetering, M., and Clevers, H. (2011). Paneth cells constitute the niche for Lgr5 stem cells in intestinal crypts. Nature *469*, 415–418.

Takeda, N., Jain, R., LeBoeuf, M.R., Wang, Q., Lu, M.M., and Epstein, J.A. (2011). Interconversion between intestinal stem cell populations in distinct niches. Science *334*, 1420–1424.

Tao, S., Tang, D., Morita, Y., Sperka, T., Omrani, O., Lechel, A., Sakk, V., Kraus, J., Kestler, H.A., Kuhl, M., et al. (2015). Wnt activity and basal niche position sensitize intestinal stem and progenitor cells to DNA damage. EMBO J. *34*, 624–640.

Tetteh, P.W., Basak, O., Farin, H.F., Wiebrands, K., Kretzschmar, K., Begthel, H., van den Born, M., Korving, J., de Sauvage, F., van Es, J.H., et al. (2016). Replacement of lost Lgr5-positive stem cells through plasticity of their enterocyte-lineage daughters. Cell Stem Cell *18*, 203–213.

Tian, H., Biehs, B., Warming, S., Leong, K.G., Rangell, L., Klein, O.D., and de Sauvage, F.J. (2011). A reserve stem cell population in small intestine renders Lgr5-positive cells dispensable. Nature *478*, 255–259.

van der Flier, L.G., van Gijn, M.E., Hatzis, P., Kujala, P., Haegebarth, A., Stange, D.E., Begthel, H., van den Born, M., Guryev, V., Oving, I., et al. (2009). Transcription factor achaete scute-like 2 controls intestinal stem cell fate. Cell *136*, 903–912.

van Es, J.H., Sato, T., van de Wetering, M., Lyubimova, A., Nee, A.N., Gregorieff, A., Sasaki, N., Zeinstra, L., van den Born, M., Korving, J., et al. (2012). Dll1+ secretory progenitor cells revert to stem cells upon crypt damage. Nat. Cell Biol. *14*, 1099–1104.

Wong, M.H., Stappenbeck, T.S., and Gordon, J.I. (1999). Living and commuting in intestinal crypts. Gastroenterology *116*, 208–210.

Wong, V.W., Stange, D.E., Page, M.E., Buczacki, S., Wabik, A., Itami, S., van de Wetering, M., Poulsom, R., Wright, N.A., Trotter, M.W., et al. (2012). Lrig1 controls intestinal stem-cell homeostasis by negative regulation of ErbB signalling. Nat. Cell Biol. *14*, 401–408.

Xian, L., Georgess, D., Huso, T., Cope, L., Belton, A., Chang, Y.T., Kuang, W., Gu, Q., Zhang, X., Senger, S., et al. (2017). HMGA1 amplifies Wnt signalling and expands the intestinal stem cell compartment and paneth cell niche. Nat. Commun. *8*, 15008.

Yan, K.S., Chia, L.A., Li, X., Ootani, A., Su, J., Lee, J.Y., Su, N., Luo, Y., Heilshorn, S.C., Amieva, M.R., et al. (2012). The intestinal stem cell markers Bmi1 and Lgr5 identify two functionally distinct populations. Proc. Natl. Acad. Sci. USA *109*, 466–471.

You, J., Zhang, Y., Li, Z., Lou, Z., Jin, L., and Lin, X. (2014). *Drosophila* perlecan regulates intestinal stem cell activity via cell-matrix attachment. Stem Cell Reports *2*, 761–769.

Yousefi, M., Li, N., Nakauka-Ddamba, A., Wang, S., Davidow, K., Schoenberger, J., Yu, Z., Jensen, S.T., Kharas, M.G., and Lengner, C.J. (2016). Msi RNA-binding proteins control reserve intestinal stem cell quiescence. J. Cell Biol. *215*, 401–413.